Functionalization of cotton nonwoven with cyclodextrin/lawsone inclusion complex nanofibrous coating for antibacterial wound dressing

Mohsen Alishahi [a], Mahmoud Aboelkheir [a], Rimi Chowdhury [b], Craig Altier [b], Hongqing Shen [c], Tamer Uyar [a,*]

[a] Fiber Science Program, Department of Human Centered Design, College of Human Ecology, Cornell University, Ithaca, NY 14853, United States
[b] Department of Population Medicine and Diagnostic Sciences, College of Veterinary Medicine, Cornell University, Ithaca, NY 14853, United States
[c] Cotton Incorporated, Cary, NC 27513, United States

ARTICLE INFO

ABSTRACT

Functionalizing cotton to induce biological activity is a viable approach for developing wound dressing. This study explores the development of cotton-based wound dressing through coating with biologically active nanofibers. Bioactive compounds like lawsone offer dual benefits of wound healing and infection prevention, however, their limited solubility and viability hinder their applications. To address this, Hydroxypropyl-beta-cyclodextrin (HP-β-CD) and Hydroxypropyl-gamma-cyclodextrin (HP-γ-CD) were employed. Inclusion complexations of CD/lawsone were achieved at 2:1 and 4:1 M ratios, followed by the fabrication of CD/lawsone nanofibrous systems via electrospinning. Phase solubility studies indicated a twofold increase in lawsone water-solubility with HP-β-CD. Electrospinning yielded smooth and uniform nanofibers with an average diameter of ~300–700 nm. The results showed that while specific crystalline peaks of lawsone are apparent in the samples with a 2:1 M ratio, they disappeared in 4:1, indicating complete complexation. The nanofibers exhibited ~100 % loading efficiency of lawsone and its rapid release upon dissolution. Notably, antibacterial assays demonstrated the complete elimination of *Escherichia coli* and *Staphylococcus aureus* colonies. The CD/lawsone nanofibers also showed suitable antioxidant activity ranging from 50 % to 70 %. This integrated approach effectively enhances lawsone's solubility through CD complexation and offers promise for bilayer cotton-based wound dressings.

1. Introduction

Wound management represents a pivotal challenge in healthcare, requiring continuous innovation and research. Wound healing is a complex procedure involving various phases such as hemostasis, inflammation, proliferation, and remodeling (Ghiyasi et al., 2023). Factors such as desiccation, infection, necrosis, pressure, and trauma can hinder the wound-healing process (Thomas, 2011). Therefore, a potent wound dressing should besides preserving the wounds from the outer environment, moisturize the skin and prevent infections (Maaz Arif et al., 2021). In this approach, smart wound dressings should not only expedite the healing process but also proactively combat infections, thereby minimizing complications and enhancing patient outcomes.

Cotton as the most dominant cellulosic fiber, has been a cornerstone in medical dressings for over a century, driven by its biocompatibility, intricate structure, moisture retention, comfort properties, and sustainable sourcing (Pinho and Soares, 2018). Although cotton gauze stands as a foundational wound dressing, its limited biological properties and drawbacks such as wound dehydration and bacterial proliferation, necessitate innovative enhancements (Pinho and Soares, 2018; Dhivya et al., 2015). Coating the cotton substrate with a biologically active layer presents a promising approach to fortifying cotton as the outer layer and another layer to facilitate wound healing and prevent infection. In this pursuit, coating nanoparticles (Montaser et al., 2020), hydrogel (Gunes and Ziylan, 2021), and nanofibers (Li et al., 2019) onto cotton substrates has emerged as a transformative strategy. Nanofibers, in particular, have garnered attention due to their resemblance to the extracellular matrix and their potential to emulate skin structure, rendering them invaluable in skin regeneration studies (Rezaei et al., 2022; Law et al., 2017). Their unique attributes, including high surface-to-volume ratio, customizable release profiles, and flexibility to be fabricated with different materials make nanofibers suitable devices for transdermal drug delivery (Asgari et al., 2021; Mendes et al., 2016).

Nanofibrous systems are especially beneficial for coating systems

with low-soluble drugs. For fast-dissolving systems and low-soluble drugs, nanofibers with their high surface-to-volume ratio can provide a higher dissolution rate (Balusamy et al., 2020; Kamali et al., 2022). Moreover, nanofibers can act as a potent system to improve drug solubility by preventing premature degradation and enabling the fast wetting and/or disintegration of its dosage form (Kajdič et al., 2020). The high surface-to-volume ratio of the nanofibers can particularly be beneficial for coating systems as they can provide a higher surface area on the first layer. Besides these advantageous features, due to the stability of the jet, producing homogenous nanofibers, and using electrostatic forces that prevent the clumping of fibers, electrospinning results in the formation of uniform nanofibrous coating and preservation of the therapeutics structure throughout the fiber formation process (Berkland et al., 2004; Zhou et al., 2009).

Several reports studied the development of nanofibers-coated cotton as a drug delivery system for wound healing applications. Moazzami Goudarzi et al. facilitated the controlled release of ciprofloxacin, clotrimazole, and benzalkonium chloride by coating the nanofibers on cotton (Moazzami Goudarzi et al., 2022). Notably, as the pursuit of optimal wound management extends beyond single-agent interventions, sometimes dual drug delivery systems should be considered. Moreover, the emergence of antibiotic-resistant bacteria has heightened the urgency to explore novel approaches that can effectively prevent infections and expedite wound closure (Davani et al., 2021; Martínez-Pérez et al., 2023). Natural bioactive agents hold promise in achieving this dual objective, given their biocompatibility, low toxicity, and multifunctional attributes, which can translate into the development of biofunctional wound dressings (Dias et al., 2011; Gaspar-Pintiliescu et al., 2019; Gorain et al., 2022). Lawsone, a naphthoquinone found abundantly in henna leaves (*Lawsonia inermis*), has garnered attention for its diverse therapeutic properties (Singh et al., 2015). Its antioxidant activity, anti-inflammatory effects, and antimicrobial attributes make it an intriguing prospect for wound management (Sakthiguru and Sithique, 2020; Jridi et al., 2017). It was shown that incorporating lawsone into chitosan/polyethylene oxide nanofibers not only introduced an antithetical property but also reduced the dressing's cytotoxicity, promoting the cell viability of normal human fibroblast cells (Abadehie et al., 2021). Another study indicated that lawsone antibacterial activity aided wound closure and accelerated wound healing in rat models (Sultana et al., 2021). It was also shown that incorporating lawsone into the nanofibers can promote wound healing by increasing the expressions of *TGF-B1* and *COL1* genes as well as enhancing re-epithelialization (Adeli-Sardou et al., 2019).

However, the clinical translation of natural bioactive agents particularly lawsone, is encumbered by challenges, including limited solubility and bioavailability. Cyclodextrins (CDs), cyclic oligosaccharides with a hydrophobic core and hydrophilic exterior, are renowned for their ability to form non-covalent inclusion complexes (Wang et al., 2023; Celebioglu and Uyar, 2020). This interaction enhances solubility, stability, and bioavailability, offering a promising avenue for elevating lawsone's therapeutic impact (Patil et al., 2023). Moreover, these molecules are particularly well-tolerated by the human body (Hsiung et al., 2022). Furthermore, the compatibility of CDs with electrospinning technology underscores their suitability for nanofiber coating on cotton substrates, amplifying their potential in wound dressing applications. The potential of the CD inclusion complexation to enhance the therapeutic efficacy of bioactives has garnered significant attention and validation across diverse research endeavors (Ertan et al., 2023; Celebioglu et al., 2022; Celebioglu et al., 2022). Thus, developing inclusion complexion with cyclodextrin (CD) is a potent approach to increase the solubility and provide stability to lawsone, and prepare nanofibrous coating on the cotton substrate for wound dressing applications. Particularly, it was shown that inclusion complexation with CDs can result in the significant improvement of the antifungal and antiparasitic activities of lawsone, upon increasing its solubility (Nicoletti et al., 2023).

Utilizing the aforementioned features of CDs, the current study aimed to prepare the inclusion complexation of lawsone and hydroxypropyl-beta-cyclodextrin (HP-β-CD) and hydroxypropyl-gamma-cyclodextrin (HP-γ-CD), and then fabrication of nanofibers to be coated on cotton substrate to develop bilayer wound dressing (Fig. 1). This approach offers the opportunity to utilize the full potential of lawsone to functionalize cotton. The morphological, structural, biological, and pharmaco-technical properties of these electrospun nanofibrous films were analyzed through appropriate techniques and approaches.

2. Materials and methods

2.1. Materials

Hydroxypropyl-beta-cyclodextrin (HP-β-CD) (Cavasol W7 HP, with a degree of substitution of approximately 0.9) and Hydroxypropyl-gamma-cyclodextrin (HP-γ-CD) (Cavasol W8 HP Pharma, with a degree of substitution of approximately 0.6) were generously provided by Wacker Chemie AG (USA) for laboratory experiments. Lawsone (2-Hydroxy-1,4-naphthoquinone, >98 %, TCI chemicals), methanol (≥99.8 % (GC), Sigma Aldrich), 2,2-diphenyl-1-picrylhydrazyl (DPPH, ≥97 %, TCI America), dimethyl sulfoxide (DMSO, >99.9 %, Sigma Aldrich), sodium chloride (NaCl, >99 %, Sigma Aldrich), potassium phosphate monobasic (KH$_2$PO$_4$, ≥99.0 %, Fisher Chemical), sodium phosphate dibasic heptahydrate (Na2HPO4, 98.0–102.0 %, Fisher Chemical), o-phosphoric acid (85 % (HPLC), Fisher Chemical), deuterated dimethylsulfoxide (d6-DMSO, 99.8 %, Cambridge Isotope), and phosphate-buffered saline tablet (PBS, Sigma Aldrich) were purchased and utilized without further purification. High-quality distilled water obtained from the Millipore Milli-Q ultrapure water system (Millipore, USA) was used in the experiments. Cotton nonwoven samples (50 GSM 100 % cotton, carded and hydroentangled substrates) were received as prototype samples from Cotton Incorporated (Cary, NC, United States).

2.2. Preparation of the solutions and electrospinning

The highly concentrated (150 % and 160 % (w/v)) and clear solutions of hydroxypropyl-beta-cyclodextrin (HP-β-CD) and hydroxypropyl-gamma-cyclodextrin (HP-γ-CD) were prepared in distilled water (0.5 mL). Next, lawsone powder was added to both HP-β-CD and HP-γ- CD solutions. At first, the concentration of the lawsone was adjusted in a way to have a 1:1 M ratio with the CDs. However, electrospinning could not be performed with this concentration. Thus, for each CD two concentrations of 4:1 and 2:1 was prepared, and the samples were named HP-β-CD/lawsone 4:1, HP-γ-CD/lawsone 4:1, HP-β-CD/lawsone 2:1, and HP-γ-CD/lawsone 4:1. The solution stirred overnight in 37 °C to form inclusion complexes. Next, the solution rested for an hour to cool down to room temperature and oust the microbubbles.

The electrospinning process was conducted using electrospinning equipment (Spingenix, model: SG100-CSS1000, Palo Alto, USA). The above-mentioned solutions were individually loaded into plastic syringes fitted with 27 G metal needles. The solutions were then extruded through the needles using a syringe pump at a flow rate of 0.5 mL/h. A grounded metal collector covered with aluminum foil was positioned 13 cm away from the needle tip to collect the electrospun webs. A stable voltage of 18 kV was applied using a high-voltage power supply. For the preparation of cotton-coated dressings, non-woven cotton was wrapped on the collector instead of aluminum foil, and electrospinning was performed using optimum conditions. The ambient conditions during the electrospinning process were recorded as 20 °C temperature and 25 % humidity. Besides nanofibrous webs, the physical mixtures (PM) of lawsone with HP-β-CD and HP-γ- CD powders having the same molar ratio of 4:1 (CD:lawsone) were also formed by blending lawsone and each cyclodextrin powder till having homogenous mixtures.
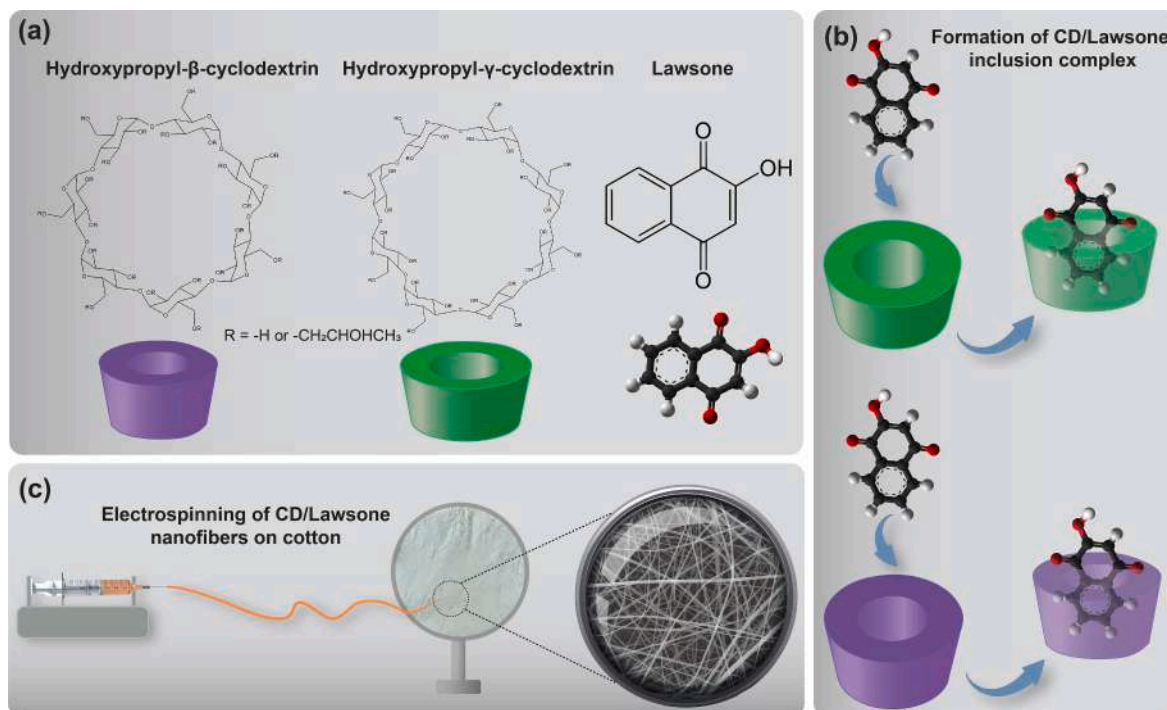
Fig. 1. The concept of study. a) Chemical structures of HP-β-CD, HP-γ-CD, and lawsone b) Schematic representation of inclusion complex formation between lawsone and HP-β-CD and HP-γ-CD molecules c) Electrospinning of CD/lawsone fibers on cotton nonwoven.

2.3. Solutions' properties

The conductivity of the electrospinning solutions was assessed at room temperature using a conductivity meter (FiveEasy, Mettler Toledo, USA). The viscosity of the same solutions was determined using a rheometer (AR 2000 rheometer, TA Instrument, USA) equipped with a 20 mm cone/plate accessory (CP 20–4 spindle type, 4°). The viscosity measurements were conducted within a shear rate range of 0.01–1000 s − 1 at a temperature of 22 °C.

2.4. Morphological analysis

The morphologies of HP-β-CD/lawsone 4:1, HP-γ-CD/lawsone 4:1, HP-β-CD/lawsone 2:1, and HP-γ-CD/lawsone 4:1 nanofibers were examined using a scanning electron microscope (SEM, Tescan MIRA3, Czech Republic). Prior to imaging, the samples were coated with a layer of Au/Pd to prevent charging-related issues. SEM images of the nanofibers were captured using a 12 kV accelerating voltage and a 10 mm distance and subsequently processed using Image J software. The software was used to analyze randomly selected 100 nanofibers and calculate the average diameter of the fibers.

2.5. Phase solubility

The phase solubility study of lawsone/HP-β-CD and lawsone/HP-γ-CD systems was conducted using a previously reported technique (Higuchi and Connors, 1965). Excess amounts of lawsone and CD powder with concentrations ranging from 0 to 32 mM were separately added to glass vials. Subsequently, 5 mL of water was added to each vial. The sealed vials were then placed on an incubator shaker, shielded from light sources, and shaken for 24 h at 25 °C and 450 rpm. After incubation, the suspensions were filtered using 0.45 μm PTFE hydrophilic filters (Thermo Scientific, Target2). The amount of lawsone in the solutions was measured by UV–Vis spectroscopy measurements (PerkinElmer, Lambda 35) at a wavelength of 458 nm, corresponding to the calibration curve of lawsone in PBS. The experiments were conducted in triplicate (n = 3), and the average absorption results were used to construct the phase solubility diagrams. The binding constants (K_S) were calculated from the equation; $K_S = slope/S0 (1-slope)$, where S_0 is the intrinsic solubility of lawsone.

2.6. The Fourier transform infrared (FTIR) spectroscopy

The Attenuated Total Reflectance Fourier Transform Infrared (ATR-FTIR) spectra of lawsone powder, HP-β-CD/lawsone 4:1, HP-γ-CD/lawsone 4:1, HP-β-CD/lawsone 2:1, and HP-γ-CD/lawsone 4:1 nanofibers were acquired using an ATR-FT-IR spectrometer (PerkinElmer, USA). The spectra were recorded in the wavenumber range of 4000 to 600 cm^{-1} with a resolution of 4 cm^{-1}, and an average of 64 scans were performed for each measurement.

2.7. Encapsulation efficiency and NMR analysis

To determine the encapsulation efficiency (%) of lawsone in CD/lawsone nanofibers samples, a certain amount of each nanofibrous sample was dissolved in dimethyl sulfoxide (DMSO), and the lawsone content in the webs was measured using UV–Vis spectroscopy. A calibration curve of lawsone in DMSO was constructed, demonstrating linearity and acceptability with an $R2 \geq 0.99$. The experiments were conducted three times, and the results were expressed as mean ± standard deviation. The encapsulation efficiency (%) (EE) was calculated using the following equation:

EE (%) = (C_e / C_t) × 100.

Where C_e represents the lawsone content on the web and C_t represents the total amount of lawsone used. For further investigation, proton nuclear magnetic resonance (^{1}H NMR, Bruker AV500 equipped with autosampler) analysis was done to determine the encapsulation efficiency (%) and molar ratio between lawsone and CD in HP-β-CD/lawsone and HP-γ-CD/lawsone nanofibrous samples. The samples along with HP-β-CD and HP-γ-CD pristine nanofibrous samples were dissolved in deuterated dimethyl sulfoxide (d6-DMSO) and ^{1}H NMR spectra were acquired using 16 scans per sample. Mestranova software was used to

investigate the spectra as the recorded spectra were subjected to base-line correction, and chemical shifts (δ, ppm) were accurately integrated. The molar ratios of HP-β-CD/lawsone and HP-γ-CD/lawsone nanofibers were determined using the signal corresponding to the –CH$_3$ protons of CD, which resonated at 1.03 ppm, and the protons associated with lawsone, which exhibited chemical shifts in the range of 6.1 to 8.00 ppm.

Rotating frame Overhauser Effect Spectroscopy (ROESY) experiments were also performed to further confirm the formation of inclusion complexes of HP-β-CD/lawsone, and HP-γ-CD/lawsone using a 600 MHz Varian INOVA nuclear magnetic resonance spectrometer in D2O at 25 °C.

2.8. X-ray diffraction (XRD)

The X-ray diffraction (XRD) patterns of lawsone powder as well as HP-β-CD/lawsone 4:1, HP-γ-CD/lawsone 4:1, HP-β-CD/lawsone 2:1, and HP-γ-CD/lawsone 4:1 nanofibers were obtained using an X-ray diffractometer (XRD, Bruker D8 Advance ECO). Prior to the measurements, the voltage was set to 40 kV and the current was set to 25 mA. Cu-Kα radiation was utilized to record the XRD patterns within the 2θ angle range of 5° to 30°.

2.9. Differential scanning calorimeter (DSC)

The thermal properties of lawsone powder as well as HP-β-CD/lawsone 4:1, HP-γ-CD/lawsone 4:1, HP-β-CD/lawsone 2:1, and HP-γ-CD/lawsone 4:1 nanofibers were analyzed using a differential scanning calorimeter (DSC, Q2000, TA Instruments, USA). Prior to the DSC measurements, the samples were accurately weighed and sealed into Tzero aluminum pans. The samples were then subjected to heating from 0 °C to 240 °C at a heating rate of 10 °C/min under a nitrogen atmosphere.

2.10. Thermogravimetric analysis

The thermogravimetric profiles of lawsone powder and CD/lawsone nanofibrous samples were analyzed using a thermogravimetric analyzer (TGA, Q500, TA Instruments, USA). For the TGA measurements, a specific weight of each sample was placed on a platinum TGA pan and heated from room temperature to 700 °C at a heating rate of 10 °C/min under a nitrogen atmosphere.

2.11. Antioxidant activity

The antioxidant activities of lawsone powder as well as HP-β-CD/lawsone 4:1, HP-γ-CD/lawsone 4:1, HP-β-CD/lawsone 2:1, and HP-γ-CD/lawsone 4:1 nanofibers were evaluated using the DPPH radical scavenging technique. For the antioxidant experiments, approximately 30 mg of the nanofibrous webs, and 3 mg of lawsone powder were individually stirred in 2 mL of distilled water at 150 rpm for 1 h. Subsequently, all aqueous systems were filtered using a 0.45 μm PTFE filter to remove any undissolved lawsone particles. Next, 1 mL of the filtered sample solution was mixed with 2 mL of 75 μM concentrated methanolic DPPH solution and incubated in the dark. UV–visible measurements were conducted at different time intervals, and the decrease in DPPH absorption at 517 nm was monitored to assess the inhibition performance of the samples. Each experiment was performed three times, and the radical scavenging performance of the samples was quantified as the inhibition percentage using the following equation:

Inhibition (%) = ((A$_{control}$ - A$_{sample}$) / A$_{control}$)* 100.

Here, A$_{control}$ represents the absorbance value of the control DPPH solution, and A$_{sample}$ represents the absorbance value of the sample solution.

2.12. In vitro release

The releasing profile of the HP-β-CD/lawsone 4:1 and HP-γ-CD/lawsone 4:1 nanofibrous samples as well as cotton nonwoven substrates coated with these nanofibrous coatings were investigated by time-dependent in vitro release. In this respect, for self-standing nanofibrous webs weighing around 10 mg were immersed in a solution of 10 mL of PBS with a pH of 7.4. The samples were placed on an orbital shaker operating at 200 rpm and maintained at a temperature of 37 °C. For nanofibrous-coated cotton samples, the same amount of 20 mg of each sample was placed in 10 mL PBS (pH = 7.4) solution and shaken with an orbital shaker at 200 rpm at 37 ∘C. At specific time intervals, 700 μl aliquots were extracted from each sample and replaced with 700 μl of fresh PBS buffer. The absorbance spectra were measured at a wavelength of 458 nm using UV spectroscopy, and the entire experiment was performed in triplicate (n = 3). The cumulative release of lawsone was investigated by evaluating the amount in each sample.

2.13. Antibacterial activity

The antibacterial activities of the nanofibers against gram-negative *Escherichia coli* (*E. coli*) and gram-positive *Staphylococcus aureus* (*S. aureus*) were analyzed by colony counting method. In this respect, the bacteria species were grown overnight without antibiotics in five ml Luria-Bertani (LB) media at 37 °C with aeration at 200 RPM. Saturated cultures were sub-cultured at a 1:100 ratio in LB media and grown at 37 °C with aeration to 1 OD (10^9 CFU/ml). Cultures were diluted in one ml LB media to the final concentration of 10^7 CFU/ml. 50 mg of each nanofibrous sample was UV sterilized and dissolved in 1 mL of the bacterial solution. An untreated sample and a sample treated with 250 μg/ml of the antibiotic streptomycin were used as the negative and positive controls, respectively. The samples were incubated at 37 °C for 24 h and after incubation, they were diluted in PBS and 100 μl were spread on LB agar plates for enumeration. The number of colonies on each plate was counted and the antimicrobial activity of each sample was calculated with respect to the negative control.

3. Results and discussion

3.1. Phase solubility

The phase solubility was conducted as described by Higuchi and Connors (Higuchi and Connors, 1965), and the results demonstrate the impact of inclusion complexation on the solubility of lawsone. The phase solubility diagrams of HP-β-CD/lawsone and HP-γ-CD/lawsone systems (Fig. 2) indicate that the bioactive solubility increased linearly. This linearity shows an A$_L$-type pattern, indicative of the formation of inclusion complexes with a 1:1 M ratio (Higuchi and Connors, 1965). The results show that the solubility of lawsone increased by ~2.18 and ~1.44 orders with inclusion complexations with HP-β-CD and HP-γ-CD, respectively. This finding aligns with previous research by Francis and Xavier, who also studied the inclusion complexation of lawsone with β-CD (Francis and Xavier, 2022).

The binding constants of lawsone (Ks) for HP-β-CD and HP-γ-CD were calculated as 394 M^{-1} and 155 M^{-1}, respectively., which shows the higher stability of HP-β-CD/lawsone inclusion complexation. These data are aligned with other studies about the inclusion complexation of lawsone with HP-β-CD (Nicoletti et al., 2023). As Fig. 2 shows, HP-β-CD formed more favorable and stable inclusion complexes with lawsone, which can be attributed to the better size match. The better size match between lawsone and HP-β-CD seems to play a crucial role in forming more favorable and stable inclusion complexes, leading to increased solubility. It has been reported that a proportional match between the agent and the CD cavity can result in better encapsulation and improved solubility (Celebioglu et al., 2022). For comparison, curcumin, another bioactive compound, showed higher solubility when encapsulated in
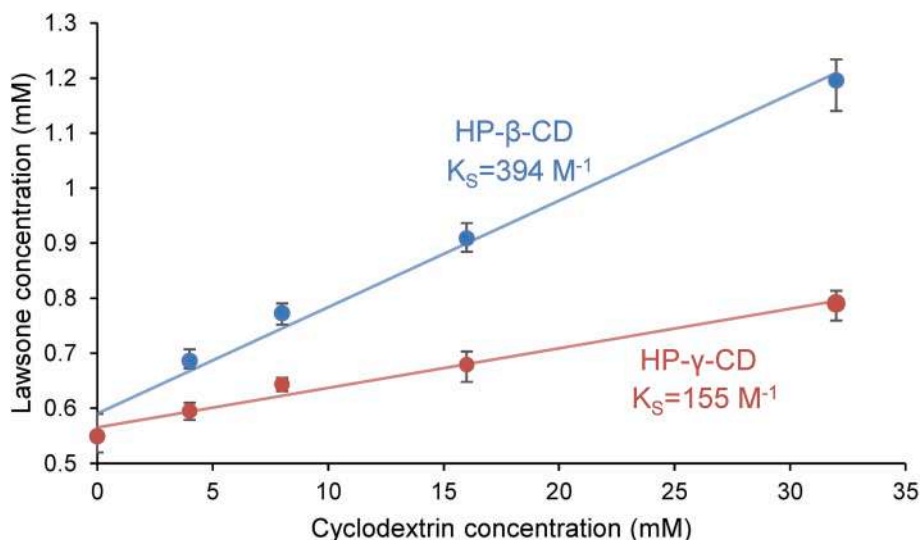
Fig. 2. Phase solubility diagram of lawsone against increasing HP-β-CD and HP-γ-CD concentrations.

HP-γ-CD, since it has a higher molecular size compared to lawsone (Celebioglu and Uyar, 2020). The successful encapsulation of lawsone within the CD cavity enhances its solubility and bioavailability, which holds significant potential for better topical activity when used as a coating for cotton substrates. The increased solubility and bioavailability through CD inclusion can translate into improved efficacy in medical applications, overcoming the hurdle of poor solubility.

3.2. Electrospinning and morphological investigation

The inclusion complexations of lawsone with HP-β-CD and HP-γ-CD were prepared in different molar ratios. Initially, different molar ratios of CDs/lawsone complexes were prepared, and it was observed that the 1:1 M ratio showed low yield and productivity in producing nanofibers. As a result, the HP-β-CD/lawsone and HP-γ-CD/lawsone complexations with 2:1 and 4:1 M ratios were chosen for the fabrication of nanofibers. Fig. 3 depicts the prepared solutions and as shown the solutions with CD/lawsone 2:1 M ratio are turbid, while the ones with 4:1 M ratio are clear, showing complete encapsulation of lawsone into the CD cavity solubilizing completely in water. However, there are still undissolved lawsone in the solution with a 2:1 M ratio. Table 1 presents the CD concentration, viscosity, conductivity, and average diameters of the fabricated fibers. The SEM images in Fig. 3 show that all the prepared nanofibers exhibited smooth and uniform morphology.

The CD/lawsone 4:1 solutions yield clearer solutions and better productivity in forming nanofibers for the electrospinning process and produce self-standing nanofibrous webs compared to the CD/lawsone 2:1 solutions. As given in Table 1, HP-β-CD/lawsone 2:1 solution with 150 % concentration yielded the thinner nanofibers, while the other concentrations at 160 % had higher viscosity and produced nanofibers with larger diameters. Accordingly, the pristine HP-β-CD fibers were smaller than those of HP-γ-CD fibers as they possessed lower viscosity and higher conductivity, in agreement with other results about the comparison of HP-β-CD and HP-γ-CD solutions (Celebioglu and Uyar, 2020). The lower viscosity due to decreased entanglement and higher conductivity resulting from increased stretching force contribute to the reduction in fibers' diameter (Topuz and Uyar, 2020). This difference in size can be attributed to the number of glucose units in the CD structure, with β-CD having seven and γ-CD having eight, resulting in higher viscosity for γ-CD (Saokham and Loftsson, 2017). Moreover, the higher ordering of water around β-CD than other CDs can lead to higher conductivity, which may also contribute to the smaller fiber size (Sandilya et al., 2020).

Regarding the effect of lawsone concentration, a comparison between HP-γ-CD/lawsone 2:1 and 4:1 shows that increasing lawsone concentration decreases the viscosity and increases the conductivity of
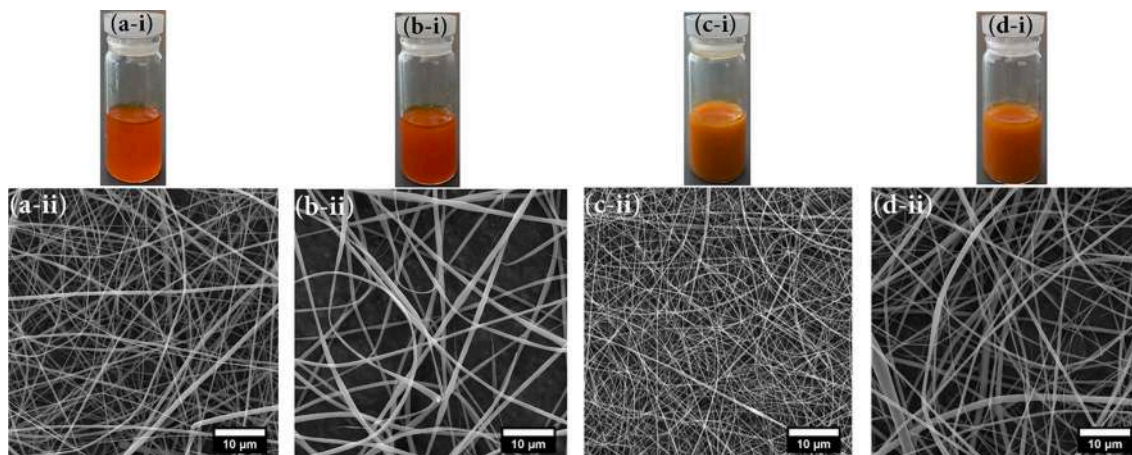

Fig. 3. i) the prepared solutions and ii) the SEM images of nanofibers a) HP-β-CD/lawsone 4:1 b) HP-γ-CD/lawsone 4:1 c) HP-β-CD/lawsone 2:1 d) HP-γ-CD/lawsone 2:1.

Table 1
The solution properties and average fiber diameters of the as-prepared fibers.

Sample	CD concentration (gr/100 mL)	Molar ratio (CD/lawsone)	Viscosity (Pa·s)	Conductivity (μS/cm)	Average fiber diameter (nm)
HP-β-CD/lawsone 4:1	160 %	4/1	0.317	134.2	430 ± 120
HP-γ-CD/lawsone 4:1	160 %	4/1	0.578	34.4	730 ± 220
HP-β-CD/lawsone 2:1	150 %	2/1	0.185	149.3	270 ± 100
HP-γ-CD/lawsone 2:1	160 %	2/1	0.468	40.1	605 ± 270

the solution, leading to smaller fiber diameters. These findings are consistent with another study that demonstrated how increasing the content of lawsone can significantly decrease fiber diameters (Abadehie et al., 2021). It was shown that lower viscosity due to lower entanglement and higher conductivity as a result of higher stretching force leads to smaller fiber diameters (Topuz and Uyar, 2020). The CD/lawsone fibers with a molar ratio of 4:1 exhibited better uniformity, which can be attributed to the formation of a more stable complexation at this molar ratio as can be seen in solutions.

Overall, the electrospinning results indicate that the choice of molar ratio in the inclusion complexation of lawsone with HP-β-CD and HP-γ-CD has a significant impact on the fabrication of nanofibers. The 4:1 M ratio showed better productivity, self-standing fibers, and improved uniformity, making it a preferable choice for the electrospinning process. Additionally, the type of CD used also influences the fiber size, with HP-β-CD resulting in smaller fibers compared to HP-γ-CD, likely due to differences in CD structure and properties.

3.3. FTIR analysis

The FTIR analysis can provide important details on the chemical interaction between the guest molecule and CD cavities. The inclusion complexation can lead to the disappearance, attenuation, or shifts in the typical FTIR peaks of guest molecules (Narayanan et al., 2017). The FTIR spectra of lawsone, and nanofibers samples (HP-β-CD/lawsone 2:1, HP-β-CD/lawsone 4:1 and HP-γ-CD/lawsone 2:1, and HP-γ-CD/lawsone 4:1) are shown in Fig. 4. Accordingly, for HP-β-CD and HP-γ-CD, the main characteristic peaks at 1019, 1080, and 1150 cm^{-1} are attributed to coupled C − C/C − O and antisymmetric C − O − C glycosidic bridge stretching (Celebioglu and Uyar, 2020). The peaks at 1366 cm^{-1} are also assigned to − CH$_3$ bending, 1646 cm^{-1} is attributed to O − H bending, 2929 cm^{-1} for C − H stretching, and 3000–3600 cm^{-1} is due to O − H stretching (Celebioglu and Uyar, 2020; Olga et al., 2015). The lawsone

spectra also showed peaks at 873 and 983 cm^{-1} due to the bending vibration of the C–H bond, peaks at 1342, 1381, and 1459 cm^{-1} attributed to the C = C, the ones at 1578 and 1593 cm^{-1} due to the stretching vibration of C = O and C = C bonds, and peaks at 1640 and 1677 cm^{-1} due to the vibration of the benzene ring (Francis and Xavier, 2022; Safie et al., 2015). The FTIR spectra of lawsone and the nanofibers were compared to investigate the inclusion complexation process and assess the encapsulation of lawsone within the CDs. Remarkably, characteristic peaks of lawsone, except those attributed to the C = C bonds, vanished in the nanofibers, while the C = C bond peaks experienced a shift from 1342 and 1459 to 1336 and 1456 cm^{-1}, respectively. However, in physical mixtures (Fig. S1), besides these peaks, the lawsone characterization peaks at 1677, 1593, 1578, 983, and 873 cm^{-1} are evident unshifted. This spectral behavior suggests that lawsone is inclusion complexed within the CD cavities, with most of its distinct peaks concealed in the FTIR spectra of nanofibers samples.

The FTIR results show that HP-β-CD and HP-γ-CD exhibited similar spectra as the main difference is the broader O − H stretching of hydroxyl groups in the HP-γ-CD spectrum. This aligns with common observations for other molecules where inclusion complexation occurs within the CD cavity, typically involving the hydrophobic region associated with the benzene ring of lawsone. (Hsu et al., 2019). The disappearance of characteristic peaks of lawsone in the FTIR spectra of the nanofibers, coupled with the shifts in the C = C bond peaks, provides compelling evidence for the successful inclusion complexation of lawsone within the CDs. These findings substantiate the notion that the inclusion complexation effectively shields lawsone within the CD cavity, which can have promising implications for the controlled release and enhanced stability of the bioactive compound.

3.4. X-ray diffraction

To gain further insights into the inclusion complexation of lawsone
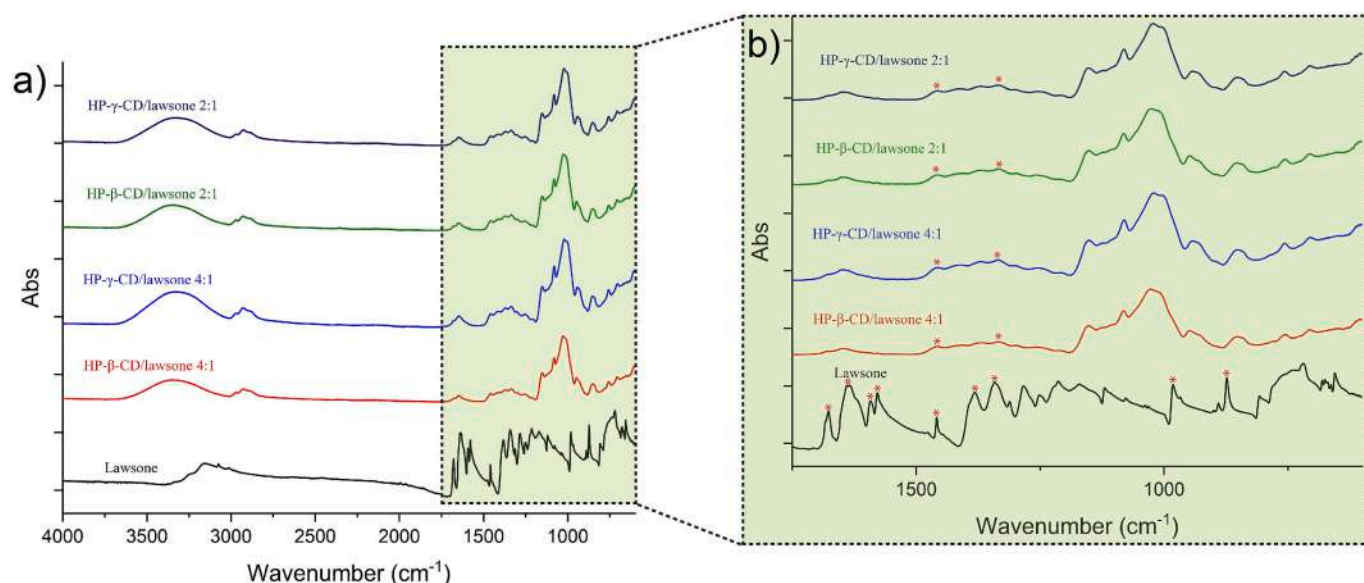

Fig. 4. a) The full and b) the expanded range FTIR spectra of the lawsone powder and as-prepared fibers. (* represents the lawsone characteristic peaks).

within the CD cavities, XRD characterization was performed, and the results are presented in Fig. 5. Lawsone is known to be a crystalline compound with characteristic peaks at 2θ values of 27.5, 23.2, 12.5, and 11.5 (Francis and Xavier, 2022). The hydroxypropylated derivatives (HP-β-CD and HP-γ-CD) are amorphous CD types, Therefore, upon inclusion complexation, the crystalline peaks of lawsone are expected to disappear due to the formation of inclusion complexes within the CD cavity and yield amorphous structure as lawsone molecules are separated from each other by CD cavity.

The XRD patterns of the nanofibers revealed interesting insights. The formation of the inclusion complexation prevented the lawsone molecules from fully forming their crystalline aggregates, as they became separated and enclosed within the cavity of the CD. For the CD/lawsone 2:1 M ratio, the characteristic peaks of lawsone were still apparent, indicating that there was some remaining amount of crystalline lawsone in this sample. However, for the CD/lawsone 4:1 M ratio, the characteristic peaks disappeared entirely, demonstrating the complete complexation of lawsone in both HP-β-CD and HP-γ-CD systems, resulting in the amorphous existence of the lawsone within the nanofibers. In comparison, in the physical mixtures (Fig. S2) all the lawsone's main crystalline peaks at 2θ values of 27.5, 23.2, 12.5, and 11.5 are presented.

These XRD findings align with the visual observations of the CD/lawsone solutions, where the solutions with a 4:1 M ratio appeared clearer compared to those with a 2:1 M ratio. The clarity of the 4:1 M ratio solution indicates the absence of undissolved lawsone crystals, unlike the 2:1 solutions which exhibited turbidity due to the presence of undissolved lawsone crystals. Comparing the characteristic peaks in samples with the 2:1 M ratio, the intensities were lower in HP-γ-CD indicating better masking the peaks due to the bigger cavity.

Overall, the XRD analysis provides robust evidence supporting the successful inclusion complexation of lawsone within the CDs at the 4:1 M ratio. The disappearance of characteristic peaks and the amorphous nature of lawsone in the nanofibers indicate that the bioactive compound is efficiently encapsulated within the CD cavities. This has significant implications for the stability and solubility of lawsone, making it a promising approach for medical applications.

3.5. DSC analysis

To further investigate the formation of inclusion complexes and the presence of uncomplexed crystalline lawsone in CD/lawsone nanofiber samples, a DSC analysis was conducted. The DSC results, depicted in Fig. 6, provide valuable insights into the thermal behavior of the samples. Specifically, the DSC curve of pure lawsone exhibits a distinct and strong peak at 198 °C, corresponding to its melting point (Sahtani et al.,
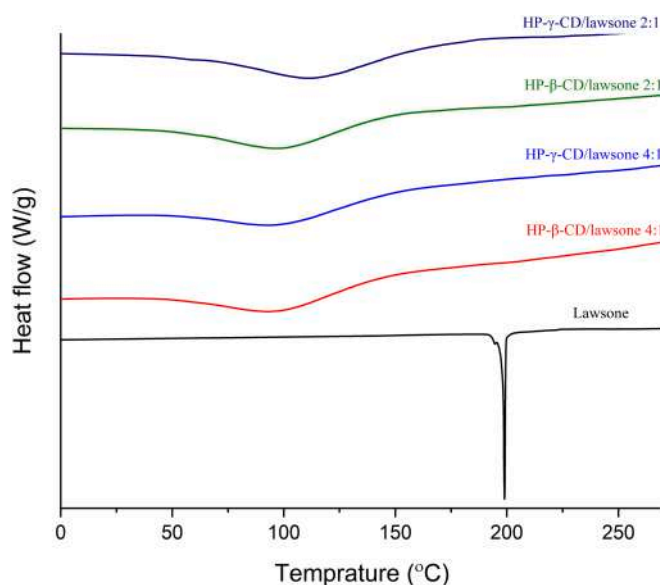

Fig. 6. DSC thermograms of lawsone powder and as-prepared nanofibers.
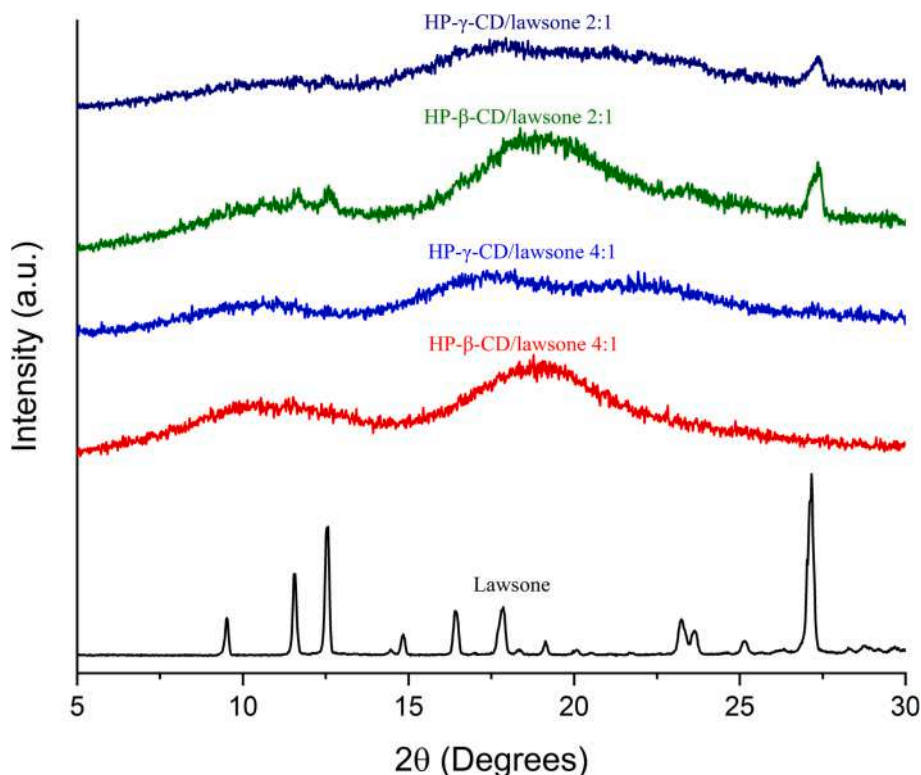

Fig. 5. XRD graphs of lawsone powder and as-prepared nanofibers.

2022). Remarkably, for all nanofiber samples, this characteristic peak of lawsone completely vanished, indicating the total encapsulation of lawsone within CDs. The absence of the lawsone peak in the DSC curves of the nanofibers corroborates the successful formation of the inclusion complex, further supporting the findings from FTIR and XRD analyses. Moreover, the broad peak observed in the DSC curves of the CD nanofibers between 30 and 130 °C is associated with the release of water molecules from the CD cavity (Hu et al., 2012). In comparison, the physical mixtures clearly show the extra peak of the lawsone melting point (Fig. S3). Accordingly, the melting point of lawsone shifted to the lower temperature ~165 °C possibly due to an eutectic relationship between lawsone and cyclodextrin resulting in the depression of the melting point to the lower temperatures (Patel and Raval, 2022).

However, it is worth noting that unlike the XRD results, the DSC curves of CD/lawsone nanofibers with a 2:1 M ratio did not exhibit the characteristic melting peak of lawsone. This disparity could be attributed to the sensitivity and resolution differences between the two techniques. XRD provides more precise information about the crystallinity of materials, while DSC offers complementary insights into the thermal properties, including melting and enthalpy changes associated with phase transitions.

3.6. TGA analysis

The thermal properties of lawsone and the nanofibrous samples were further investigated using TGA analysis, with the results depicted in Fig. 7, along with the corresponding DTG curves. Lawsone powder displayed a main degradation peak between 130 and 180 °C, followed by a minor degradation peak up to 450 °C. In contrast, the nanofiber samples exhibited a distinct thermal behavior. The characteristic degradation peak of lawsone is not presented as an independent stage, and regardless of the type of CDs used and their concentrations, the fibers demonstrated a similar trend of degradation between 350 and 400 °C. The initial degradation of the nanofibers from 30 to 100 °C (about 5 %) is attributed to dehydration. These trends coincide with the thermal behavior of pristine HP-β-CD and HP-γ-CD nanofibers, providing evidence for the complete complexation of lawsone within the CDs (Celebioglu and Uyar, 2020). Physical mixtures though showed an initial 3 % (w/w) degradation near lawsone degradation peaks at 150–180 °C followed by the main degradation stage of cyclodextrins. Accordingly, the degradation peak of lawsone is not presented in the nanofibers' curves as a separate step, which can be indicated as the enhancement of the thermal stability of lawsone by the inclusion complexation (Celebioglu and Uyar, 2020;

Celebioglu and Uyar, 2021). However, as the lawsone degradation peak is masked by the CDs, the amount of lawsone can not be evaluated by TGA.

Analyzing the DTG curves of the fibers, a slight peak was observed for the HP-β-CD/lawsone 2:1 sample between 150 and 200 °C, which is consistent with the XRD data. This peak may be indicative of the presence of a small amount of crystalline lawsone within the complexation. DTG curves of the physical mixtures (Fig. S4b) also clearly show the lawsone degradation peak. Overall, the TGA and DTG analyses provide further support for the successful inclusion complexation of lawsone within the CDs in the nanofibers. The disappearance of characteristic degradation peaks of lawsone and the presence of similar thermal behavior to pristine CD nanofibers substantiate the complete encapsulation of lawsone within the CDs.

3.7. Encapsulation efficiency

The encapsulation efficiencies of the nanofibrous samples were first determined by dissolving the nanofibrous mats in DMSO. Accordingly, the encapsulation efficiencies of HP-β-CD/lawsone 4:1 and HP-γ-CD/lawsone 4:1 samples were measured as 99.8 ± 0.9 and 99.3 ± 1.0, respectively. The efficiencies for HP-β-CD/lawsone 2:1 and HP-γ-CD/lawsone 2:1 were also 97.3 ± 1.3 and 97.1 ± 1.0, respectively. This observation implies that encapsulation efficiency was marginally higher in nanofibers with lower molar ratios, potentially indicative of the presence of non-encapsulated lawsone in samples with higher molar ratios. Importantly, these outcomes collectively indicate the near-complete encapsulation of the lawsone bioactive agent during the process of inclusion complexation and subsequent electrospinning. This phenomenon underscores the proficiency of both HP-β-CD and HP-γ-CD in achieving virtually complete encapsulation of lawsone content. To further measure the molar ratios of lawsone and CDs in the nanofibrous samples ^{1}H NMR analysis was conducted. Fig. 8 displays the ^{1}H NMR spectra of pure lawsone, HP-β-CD/lawsone, and HP-γ-CD/lawsone with 2:1 and 4:1 M ratios, as well as HP-β-CD and HP-γ-CD pristine nanofibrous samples dissolved in d-DMSO. Accordingly, considering the spectra of pristine CD fibers the unique peak at 1.03 ppm (–CH3) is assigned to identify HP-β-CD and HP-γ-CD in the fibers (Hsiung et al., 2022). Simultaneously, the characteristic peaks of lawsone were identified within the 6.1–8 ppm range, corresponding to the two rings of the lawsone molecule (as illustrated in Fig. 8(a, b)) (Miroshnikov et al., 2018), The analytical measurement showed that the molar ratio for HP-β-CD/lawsone 4:1 nanofibers was approximately 4.13/1, indicating
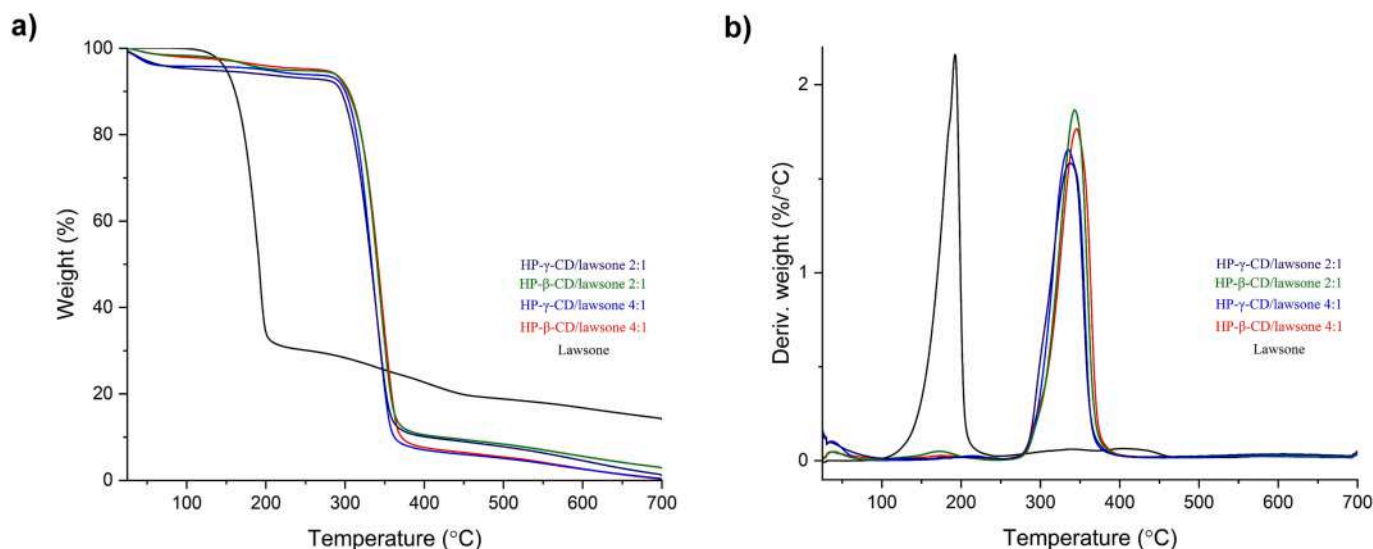

Fig. 7. a) TGA thermograms and b) the derivative graphs (DTG) of lawsone powder and as-prepared nanofibers.
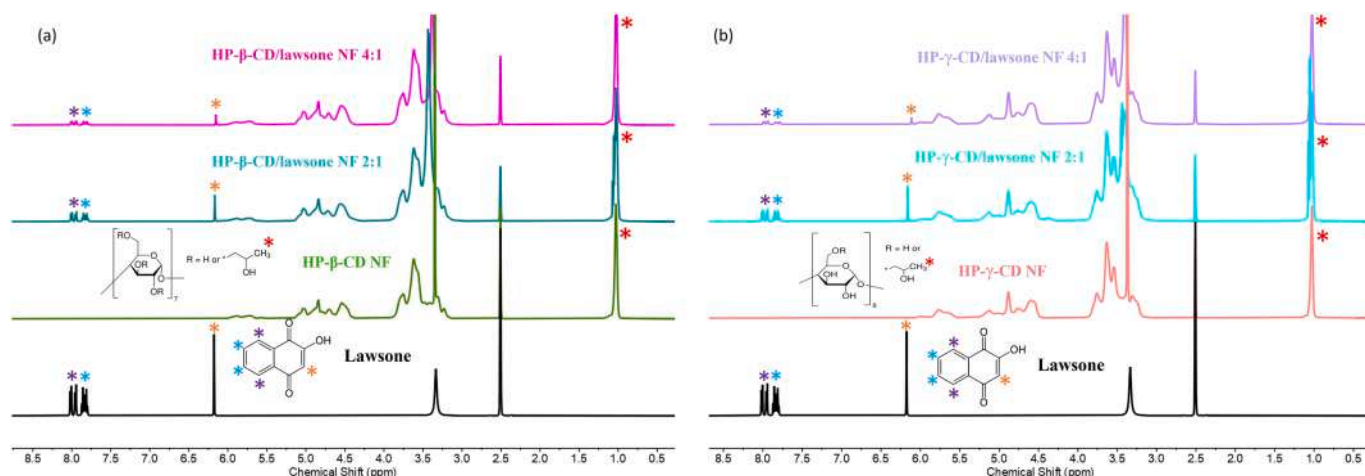
Fig. 8. (a) ^{1}H NMR spectra of lawsone and HP-β-CD/lawsone 4:1, HP-β-CD/lawsone 2:1, and pristine HP-β-CD nanofibers, (b) ^{1}H NMR spectra of lawsone and HP-γ-CD/lawsone 4:1, HP-γ-CD/lawsone 2:1, and pristine HP-γ-CD nanofibers.

almost complete preservation of the initial ratio. This result suggests an impressive loading efficiency of approximately 97 % and a final lawsone content of approximately 2.66 % (w/w) in the nanofibers. As for HP-β-CD/lawsone 2:1 nanofibers, the loading efficiency was lower at approximately 95.40 %. Compared to HP-β-CD samples, HP-γ-CD/lawsone 2:1 and 4:1 (CD/lawsone) showed reduced loading efficiencies of
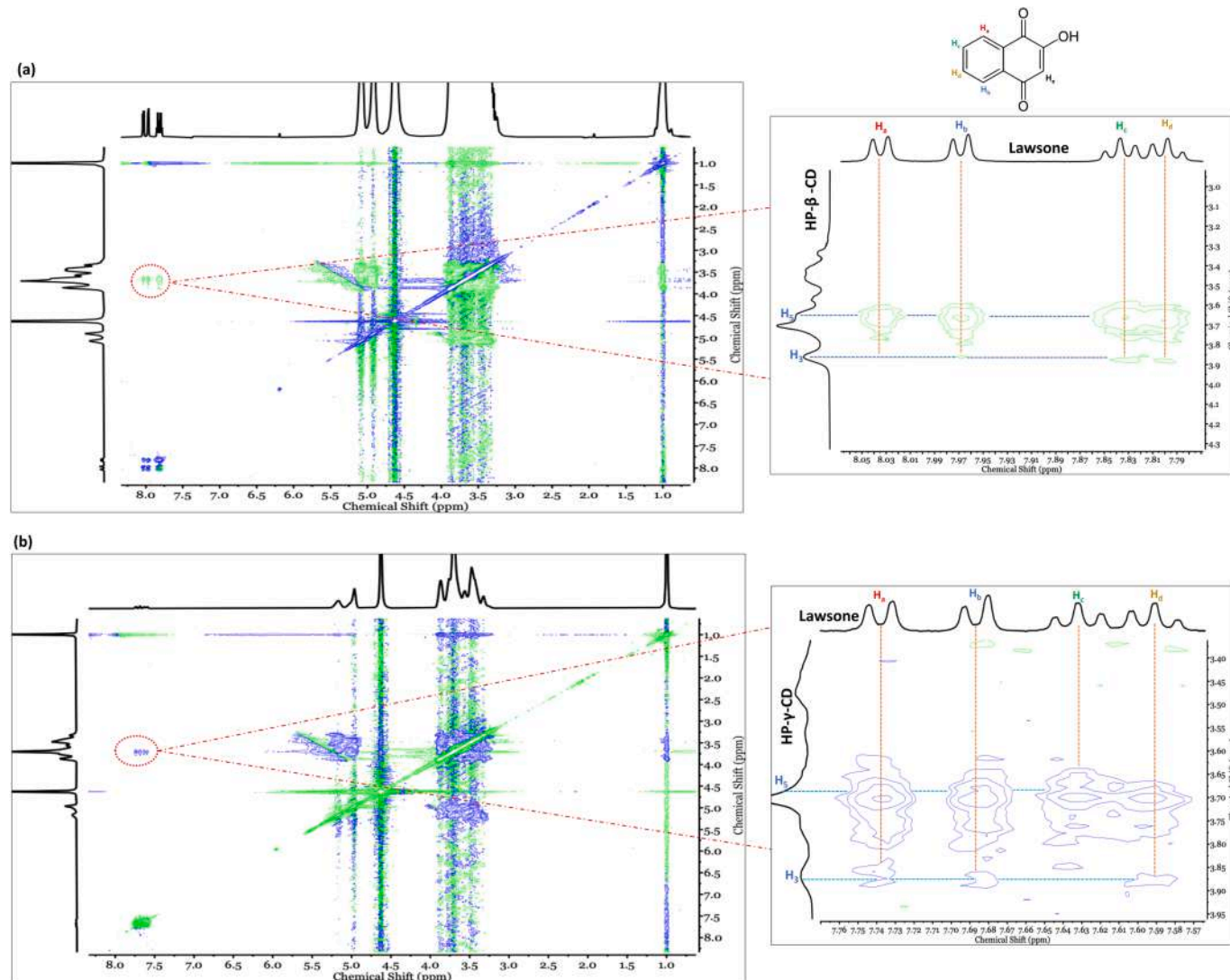

Fig. 9. 2D ROESY spectra of (a) HP-β-CD/lawsone inclusion complex, (b) HP-γ-CD/lawsone inclusion complex.

approximately 90.30 % and 91.20 %, respectively. These findings are in agreement with the result of loading efficiency that more than 90 % of lawsone encapsulated in CD. These outcomes indicate the higher encapsulation efficiency of lawsone in HP-β-CD nanofibers compared to HP-γ-CD nanofibers and in agreement with phase solubility measurement. Furthermore, The NMR spectra show that the characteristic peaks of lawsone maintained a consistent pattern in all HP-β-CD/lawsone and HP-γ-CD/lawsone nanofibrous samples, indicating the preservation of lawsone's chemical structure throughout all the preparation and electrospinning processes. These findings affirm the successful encapsulation of lawsone within the HP-β-CD and HP-γ-CD nanofibers and validate the structural integrity of the encapsulated lawsone in the nanofibers.

Nuclear Overhauser Effect Spectroscopy (NOESY) and Rotating frame Overhauser Effect Spectroscopy (ROESY) represent pivotal 2D-NMR techniques extensively applied to investigate the interactions of cyclodextrins (CDs) with a diverse range of guest molecules, encompassing organic, inorganic, and hybrid compounds. These NOE-based experiments, specifically NOESY and ROESY, are the methods of choice when delving into non-covalent interactions within supramolecular systems involving CD hosts, particularly cavitand molecules (Schneider et al., 1998; Haouas et al., 2023). By leveraging NMR techniques that rely on "through space" interactions or dipolar coupling, a profound understanding of the spatial proximity between the host and the guest components of a system can be acquired. ROESY, with its capability to probe over longer distances, reaching up to 5 Å, emerges as the preferred choice over NOESY, specifically for scrutinizing nanoscale assemblies constructed with CDs. Furthermore, the ROESY method offers the distinct advantage of yielding positive Rotating frame Overhauser Effect (ROE) signals, a characteristic feature beneficial for macromolecules and extensive chemical complexes. ROESY's aptitude to reveal NOE cross-correlation between closely situated protons, especially in the context of host–guest interactions, underscores its potential to shed light on spatial proximity, quantifiable at distances less than 0.4 nm. This attribute makes ROESY particularly suitable for offering conformational insights into the inclusion complexation phenomenon (Schneider et al., 1998; Haouas et al., 2023);

Herein, the ROESY NMR technique was successfully utilized to explore host–guest interactions occurring through space in solution between HP-β-CD and HP-γ-CD, and lawsone as shown in Fig. 9. Analysis of the ROESY spectra for the HP-β-CD/lawsone and HP-γ-CD/lawsone systems unveiled overlapping proton signals between the inner cavity protons (H_3 and H_5) of the CDs and the aromatic protons of lawsone. This observation unmistakably signifies the establishment of inclusion complexes for both cyclodextrin types with lawsone, thereby underscoring the efficacy of ROESY in capturing the essence of these host-guest interactions. In conclusion, our study leveraged ROESY NMR spectroscopy to unravel the intricate host–guest contacts occurring between cyclodextrins and lawsone in solution. This method, with its unique ability to elucidate spatial proximity and non-covalent interactions, stands as a powerful tool in the characterization of CD inclusion complexes.

3.8. Antioxidant activity

The primary objective of this study is the functionalization of cotton dressing for wound healing applications. One crucial avenue to enhance wound healing is the reduction of oxidative stress in the wound microenvironment, which can mitigate cellular damage and inflammation (Jafari et al., 2023). Notably, wound sites, especially those infected, exhibit elevated levels of free radicals, rendering them susceptible to lipid peroxidation, increased oxidative stress, DNA damage, and enzyme inactivation (Qu et al., 2018). Utilizing the antioxidant properties of lawsone, as a bioactive agent, can offer a valuable contribution to the wound healing process when integrated into a cotton-based dressing. Lawsone antioxidant property is attributed to the proton-donating capacity of its phenolic groups, which play a pivotal role in quenching free

radicals and intercepting radical chain reactions. The modulatory influence of lawsone on redox signaling through diverse pathways is also another factor in decreasing free radical-induced oxidative stress (Sakthiguru and Sithique, 2020).

The antioxidant activities of lawsone and nanofibrous samples at different times were determined and depicted in Fig. 10. Comparing the antioxidant activities, CD/lawsone nanofibers with a 2:1 M ratio showed higher antioxidant activity due to higher drug content. Among the types of cyclodextrin, the HP-β-CD showed higher activity than HP-γ-CD as considering the phase solubility results, the higher solubility of HP-β-CD/lawsone inclusion complexation can result in a higher amount of bioactive after filtration and more scavenging of DPPH radical. Besides, considering the molar ratios HP-β-CD has a lower molecular weight, and hence its fibers contain a higher amount of lawsone using a similar mat weight. Significantly, the antioxidant activity experiences a substantial augmentation with time, escalating from approximately 20 % to around 65 % for HP-β-CD/lawsone 2:1 nanofibers. This enhancement is primarily attributed to the inclusion complexation process, which substantially increases the solubility of lawsone, and consequently, its antioxidant potential.

It was shown that the encapsulation of lawsone in nanocomposite with O-Carboxymethyl chitosan and nano-zinc oxide can improve its stability, however, the antioxidant activities could not surpass that of pure lawsone (Sakthiguru and Sithique, 2020). In our study, the dual strategies of increasing solubility through inclusion complexation and employing a nanofibrous system characterized by a high surface-to-volume ratio and encapsulation efficiency resulted in markedly higher antioxidant activity compared to pure lawsone. This elevated antioxidant potential, coupled with the compound's anticipated anti-inflammatory, antipyretic, and analgesic effects, positions the functionalized cotton wound dressing as a potential device for the wound healing process (Rahmani et al., 2015).

3.9. Antibacterial activity

In addition to facilitating wound healing, an efficacious smart wound dressing must possess the capacity to prevent and eradicate infections. Infections not only impede the wound healing process, but severe cases can escalate into systemic threats with potentially fatal consequences (Huang et al., 2023; Liang et al., 2021). As a Naphthoquinone derivative, lawsone can show broad antimicrobial activities using mechanisms such as plasmid neutralization within bacteria, disruption of efflux pump functions, and inhibition of topoisomerase activity (Buckner et al., 2018; Ohene-Agyei et al., 2014; Karkare et al., 2013).

The evaluation of the nanofibrous samples' activity against prominent bacterial culprits, *E. coli* and *S. aureus*, was undertaken through meticulous colony-counting techniques. These bacterial strains are pivotal players in the genesis of wound infections and offer valuable insight into the potential of lawsone as an antimicrobial agent. Furthermore, the observations garnered from this study can provide a broader perspective on lawsone's antibacterial efficacy across aerobic gram-negative and gram-positive bacterial species. As illustrated in Fig. 11, the negative control group did not show any antimicrobial activity, allowing bacterial growth. In stark contrast, groups treated with nanofibers showed a significant reduction in the growth of both *E. coli* and *S. aureus*, demonstrating the potency of the antimicrobial activity. The growth inhibition is strikingly evident in Fig. 11, where all four nanofibrous samples achieved the complete eradication of both gram-negative and gram-positive bacteria, demonstrated by the absence of colonies on the culture plates.

The results also showed that there is no difference in the antibacterial activities between CD/lawsone molar ratios of 4:1 and 2:1, indicating fibers possessed sufficient antibacterial activity even with the lower lawsone content. It was shown that lawsone-incorporated polycaprolactone-gelatin nanofibers exhibited an inhibition zone against gram-positive bacteria across all lawsone concentrations. However, this
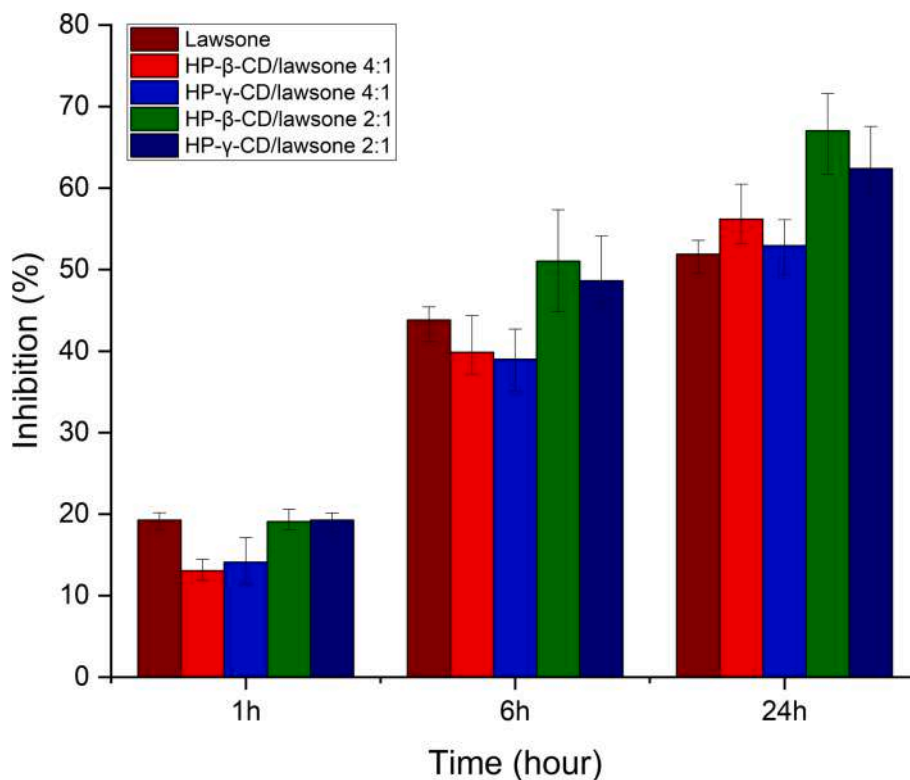
Fig. 10. The antioxidant activity of lawsone powder and as-prepared nanofibers.
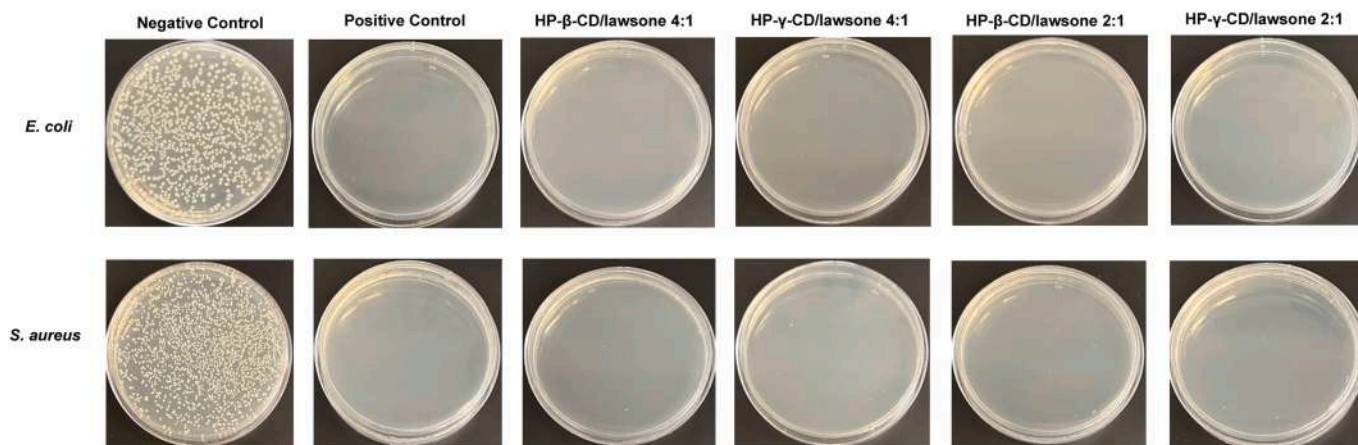

Fig. 11. Antibacterial activity of the prepared nanofibers and the control samples.

antibacterial activity against gram-negative bacteria was discernible only at the highest bioactive concentration (Adeli-Sardou et al., 2018). Same results were also obtained by incorporating lawsone in chitosan/ polyethylene oxide which showed better antibacterial activity against gram-positive bacteria (Ahmad and Beg, 2001). In our study, the inclusion complexation leading to better lawsone solubility resulted in significant activity against both gram-negative and gram-positive bacterial species.

This resounding 100 % eradication demonstrates the remarkable potential of this nanofibrous-coated cotton wound dressing as an effective strategy for managing and preventing wound infections. Furthermore, considering the conceivable activity of lawsone against additional bacterial species such as *Bacillus subtilis* and *Pseudomonas aeruginosa*, the envisaged application of this dressing extends to addressing highly infectious wounds such as diabetic ulcers (Ding et al., 2022).

3.10. In vitro release

Given the comparable antibacterial potency and slight disparity in antioxidant activities between CD/lawsone molar ratios of 4:1 and 2:1and taking into account the superior yield and morphological attributes of the lower concentration, the nanofibrous samples HP-β-CD/ lawsone 4:1 and HP-γ-CD/lawsone 4:1 emerged as the optimal candidates. Subsequently, these optimized nanofibrous samples were adeptly coated onto cotton substrates to ascertain their controlled release behavior. The cotton substrates coated with CDs/lawsone nanofibers are illustrated in Fig. 12a.

The releasing profiles of the coated cotton as well as the free-standing fibers are estimated and illustrated in Fig. 12b. A substantial portion of the lawsone content, approximately 84 % in HP-β-CD/law-sone 4:1 and 77 % in HP-γ-CD/lawsone 4:1 nanofibers was swiftly released within the initial 30 s. This pronounced initial release phase is
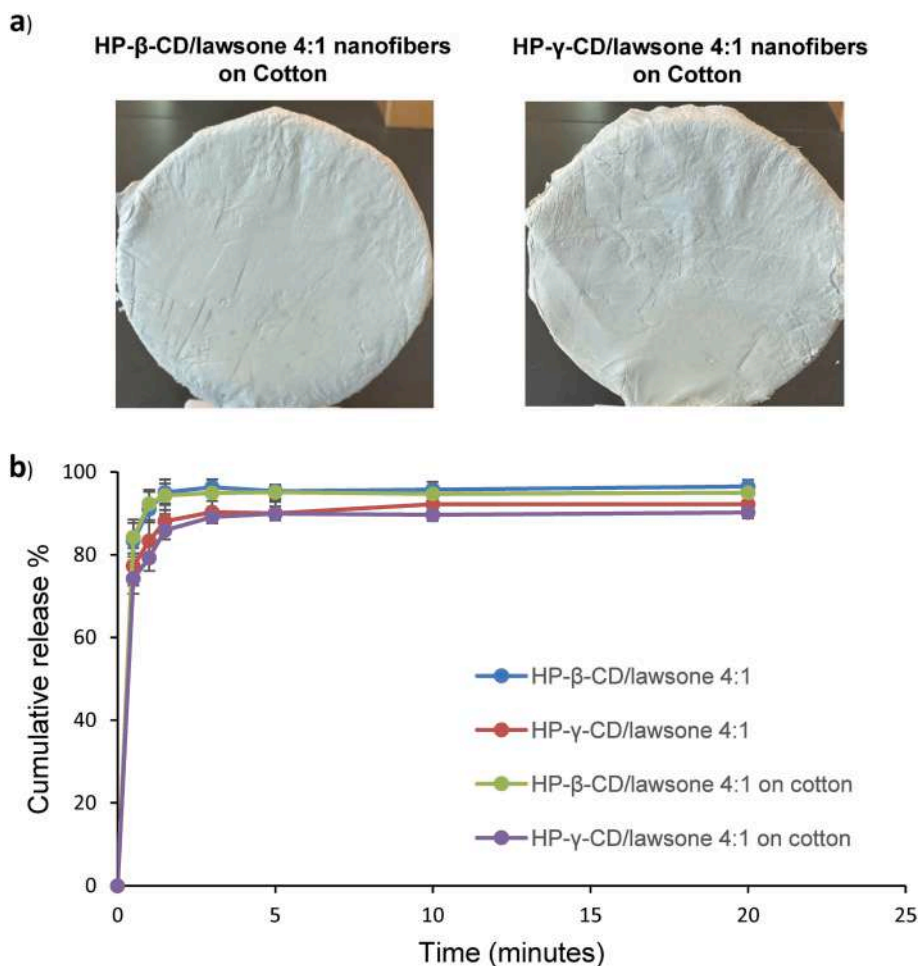
Fig. 12. a) The cotton nonwoven coated with nanofibers b) The releasing profile of free-standing nanofibers and nanofiber-coated cotton nonwoven.

attributed to the rapid dissolution of the fibers, facilitated by their inherent fast-dissolving characteristics, ultimately leading to complete dissolution within the PBS medium by the third minute. As the mechanism of release in this fast-dissolving system is through the dissolution of the fibers, lawsone was released completely after the dissolution. Furthermore, the release profile exhibited by the cotton-coated samples mirrored that of the free-standing fibers. This similarity is attributed to the absence of chemical linkage between the cotton substrate and the nanofibers. This rapid and substantial release profile holds significant promise in terms of delivering a high concentration of lawsone to wounds. This approach holds particular relevance for infected wounds, given the pronounced antibacterial activity of this system. This interplay between the encapsulation and releasing profile underscores the potential of this nanofibrous-coated cotton wound dressing as a formidable strategy for efficient and targeted wound management.

4. Conclusion

Compared to synthetic materials, cotton has many properties that make its substrate ideal for use in wound dressing including high absorbency, hypoallergenic, soft, comfortable, breathable, biodegradable, natural origin, widely available, and easy processing. When developing wound healing patches or any other medical textiles, choosing the right substrate is essential for achieving optimal performance and patient comfort. Although a foundational material in wound dressing, cotton is accompanied by inherent biological limitations. This study successfully addresses these limitations by imparting cotton with a biologically active nanofibrous layer. The integration of lawsone as a bioactive agent

holds immense potential for wound healing, yet its constrained solubility prompted the utilization of inclusion complexation with Hydroxypropyl-beta-cyclodextrin (HP-β-CD) and Hydroxypropyl-gamma-cyclodextrin (HP-γ-CD). This approach, validated by phase solubility studies, substantially increased the lawsone solubility, with HP-β-CD emerging as the superior complexation agent due to the better match of the lawsone with its cavity. The resulting uniform nanofibers showed to have almost complete encapsulation efficiency with variations attributed to the presence of non-encapsulated lawsone in higher molar ratio samples, as shown in crystalline peak analysis. The increased solubility, achieved through inclusion complexation, translated into suitable antioxidant activity, surpassing that of lawsone powder. Moreover, the nanofibers showed excellent antibacterial activity, effectively eradicating *Escherichia coli* and *Staphylococcus aureus* colonies across all samples. The similarity in antibacterial and antioxidant performance of 2:1 and 4:1 M ratios prompted the selection of the former for coating onto the cotton substrate. Notably, this coated substrate exhibited rapid release upon dissolution of the nanofiber coating. Collectively, this study advances the realm of wound management by enhancing lawsone activity through the inclusion complexation and functionalizing cotton through CD/lawsone nanofiber coatings. The integrated approach not only demonstrates a method to boost lawsone efficacy but also underscores the potential of functionalized cotton-based wound dressings. With promising antibacterial and antioxidant attributes, this innovative method holds significant promise for the development of biofunctional wound dressings with enhanced therapeutic potential.

Funding

This research was funded by Cotton Incorporated (Cary, NC, USA), Project Number: 23-887

CRediT authorship contribution statement

Mohsen Alishahi: Data curation, Formal analysis, Conceptualization, Methodology, Validation, Investigation, Writing – original draft, Writing – review & editing. **Mahmoud Aboelkheir:** Data curation, Formal analysis. **Rimi Chowdhury:** Data curation, Formal analysis. **Craig Altier:** Resources, Supervision. **Hongqing Shen:** Conceptualization, Methodology, Writing – review & editing. **Tamer Uyar:** Supervision, Resources, Conceptualization, Methodology, Formal analysis, Writing – review & editing, Project administration, and Funding acquisition.

Declaration of competing interest

The authors declare that they have no known competing financial interests or personal relationships that could have appeared to influence the work reported in this paper.

Data availability

Data will be made available on request.

Appendix A. Supplementary data

Supplementary data to this article can be found online at https://doi.org/10.1016/j.ijpharm.2024.123815.

References

Abadehie, F.S., Dehkordi, A.H., Zafari, M., Bagheri, M., Yousefiasl, S., Pourmotabed, S., et al., 2021. Lawsone-encapsulated chitosan/polyethylene oxide nanofibrous mat as a potential antibacterial biobased wound dressing. Eng. Regener. 2, 219–226.

Adeli-Sardou, M., Torkzadeh-Mahani, M., Yaghoobi, M.M., Dodel, M., 2018. Antibacterial and anti-biofilm investigation of electrospun PCL/gelatin/Lawsone nano fiber scaffolds against biofilm producing bacteria. Biomacromol. J. 4 (1), 46–57.

Adeli-Sardou, M., Yaghoobi, M.M., Torkzadeh-Mahani, M., Dodel, M., 2019. Controlled release of lawsone from polycaprolactone/gelatin electrospun nano fibers for skin tissue regeneration. Int. J. Biol. Macromol. 124, 478–491.

Ahmad, I., Beg, A.Z., 2001. Antimicrobial and phytochemical studies on 45 Indian medicinal plants against multi-drug resistant human pathogens. J. Ethnopharmacol. 74 (2), 113–123.

Asgari, Q., Alishahi, M., Davani, F., Caravan, D., Khorram, M., Enjavi, Y., et al., 2021. Fabrication of amphotericin B-loaded electrospun core–shell nanofibers as a novel dressing for superficial mycoses and cutaneous leishmaniasis. Int. J. Pharm. 606, 120911.

Balusamy, B., Celebioglu, A., Senthamizhan, A., Uyar, T., 2020. Progress in the design and development of "fast-dissolving" electrospun nanofibers based drug delivery systems - a systematic review. J. Control. Release 326, 482–509.

Berkland, C., Pack, D.W., Kim, K., 2004. Controlling surface nano-structure using flow-limited field-injection electrostatic spraying (FFESS) of poly(d, l-lactide-co-glycolide). Biomaterials 25 (25), 5649–5658.

Buckner, M.M., Ciusa, M.L., Piddock, L.J., 2018. Strategies to combat antimicrobial resistance: anti-plasmid and plasmid curing. FEMS Microbiol. Rev. 42 (6), 781–804.

Celebioglu, A., Saporito, A.F., Uyar, T., 2022. Green Electrospinning of chitosan/pectin nanofibrous films by the incorporation of cyclodextrin/curcumin inclusion complexes: ph-responsive release and hydrogel features. ACS Sustain. Chem. Eng. 10 (14), 4758–4769.

Celebioglu, A., Uyar, T., 2020. Fast-dissolving antioxidant curcumin/cyclodextrin inclusion complex electrospun nanofibrous webs. Food Chem. 317, 126397.

Celebioglu, A., Uyar, T., 2021. Electrospun formulation of acyclovir/cyclodextrin nanofibers for fast-dissolving antiviral drug delivery. Mater. Sci. Eng. C 118, 111514.

Celebioglu, A., Tekant, D., Kilic, M.E., Durgun, E., Uyar, T., 2022. Orally fast-disintegrating resveratrol/cyclodextrin nanofibrous films as a potential antioxidant dietary supplement. ACS Food Sci. Technol. 2 (3), 568–580.

Celebioglu, A., Uyar, T., 2020. Development of ferulic acid/cyclodextrin inclusion complex nanofibers for fast-dissolving drug delivery system. Int. J. Pharm. 584, 119395.

Davani, F., Alishahi, M., Sabzi, M., Khorram, M., Arastehfar, A., Zomorodian, K., 2021. Dual drug delivery of vancomycin and imipenem/cilastatin by coaxial nanofibers for treatment of diabetic foot ulcer infections. Mater. Sci. Eng. C 123, 111975.

Dhivya, S., Padma, V.V., Santhini, E., 2015. Wound dressings - a review. Biomedicine 5 (4), 22.

Dias, A.M.A., Braga, M.E.M., Seabra, I.J., Ferreira, P., Gil, M.H., de Sousa, H.C., 2011. Development of natural-based wound dressings impregnated with bioactive compounds and using supercritical carbon dioxide. Int. J. Pharm. 408 (1), 9–19.

Ding, Q., Jing, X., Yao, S., Su, W., Ye, B., Qu, Y., et al., 2022. Multifunctional hydrogel loaded with 4-octyl itaconate exerts antibacterial, antioxidant and angiogenic properties for diabetic wound repair. Biomater. Adv. 139, 212979.

Ertan, K., Celebioglu, A., Chowdhury, R., Sumnu, G., Sahin, S., Altier, C., Uyar, T., 2023. Carvacrol/cyclodextrin inclusion complex loaded gelatin/pullulan nanofibers for active food packaging applications. Food Hydrocoll. 142, 108864.

Francis, S.M., Xavier, E.N., 2022. Solubility enhancement of lawsone by complexation with beta cyclodextrin. Indian J. Pharm. Edu. Res. 56 (3), 706–715.

Gaspar-Pintiliescu, A., Stanciuc, A.-M., Craciunescu, O., 2019. Natural composite dressings based on collagen, gelatin and plant bioactive compounds for wound healing: a review. Int. J. Biol. Macromol. 138, 854–865.

Ghiyasi, Y., Prewett, P.D., Davies, G.J., Faraji, R.d.Z., 2023. The role of microneedles in the healing of chronic wounds. Int. J. Pharm. 641, 123087.

Gorain, B., Pandey, M., Leng, N.H., Yan, C.W., Nie, K.W., Kaur, S.J., et al., 2022. Advanced drug delivery systems containing herbal components for wound healing. Int. J. Pharm. 617, 121617.

Gunes, O.C., Ziylan, A.A., 2021. Antibacterial Polypeptide nisin containing cotton modified hydrogel composite wound dressings. Polym. Bull. 78, 6409–6428.

Haouas, M., Falaise, C., Leclerc, N., Floquet, S., Cadot, E., 2023. NMR spectroscopy to study cyclodextrin-based host-guest assemblies with polynuclear clusters. Dalton Trans.

Higuchi, T., Connors, K., 1965. Phase solubility diagram. Adv Anal Chem Instrum. 4, 117–212.

Hsiung, E., Celebioglu, A., Kilic, M.E., Durgun, E., Uyar, T., 2022. Ondansetron/Cyclodextrin inclusion complex nanofibrous webs for potential orally fast-disintegrating antiemetic drug delivery. Int. J. Pharm. 623, 121921.

Hsu, C.-M., Yu, S.-C., Tsai, F.-J., Tsai, Y., 2019. Characterization of in vitro and in vivo bioactivity of a ferulic acid-2-Hydroxypropyl-β-cyclodextrin inclusion complex. Colloids Surf. B Biointerfaces 180, 68–74.

Hu, L., Zhang, H., Song, W., Gu, D., Hu, Q., 2012. Investigation of inclusion complex of cilnidipine with hydroxypropyl-β-cyclodextrin. Carbohydr. Polym. 90 (4), 1719–1724.

Huang, X., Xu, L., Yu, X., Li, Y., Huang, Z., Xu, R., et al., 2023. Near-infrared light-responsive multifunctional hydrogel releasing peptide-functionalized gold nanorods sequentially for diabetic wound healing. J. Colloid Interface Sci. 639, 369–384.

Jafari, H., Ghaffari-Bohlouli, P., Alishahi, M., Davani, F., Daneshi, S.S., Heidari, R., et al., 2023. Tissue adhesive hydrogel based on upcycled proteins and plant polyphenols for enhanced wound healing. Mater. Today Chem. 33, 101722.

Jridi, M., Sellimi, S., Lassoued, K.B., Beltaief, S., Souissi, N., Mora, L., et al., 2017. Wound healing activity of cuttlefish gelatin gels and films enriched by henna (Lawsonia inermis) extract. Colloids Surf A Physicochem Eng Asp 512, 71–79.

Kajdič, S., Zupančič, Š., Roškar, R., Kocbek, P., 2020. The potential of nanofibers to increase solubility and dissolution rate of the poorly soluble and chemically unstable drug lovastatin. Int. J. Pharm. 573, 118809.

Kamali, H., Farzadnia, P., Movaffagh, J., Abbaspour, M., 2022. Optimization of curcumin nanofibers as fast dissolving oral films prepared by emulsion electrospinning via central composite design. J. Drug Delivery Sci. Technol. 75, 103714.

Karkare, S., Chung, T.T., Collin, F., Mitchenall, L.A., McKay, A.R., Greive, S.J., et al., 2013. The naphthoquinone diospyrin is an inhibitor of DNA gyrase with a novel mechanism of action. J. Biol. Chem. 288 (7), 5149–5156.

Law, J.X., Liau, L.L., Saim, A., Yang, Y., Idrus, R., 2017. Electrospun collagen nanofibers and their applications in skin tissue engineering. Tissue Eng. Regener. Med. 14, 699–718.

Li, Z., Milionis, A., Zheng, Y., Yee, M., Codispoti, L., Tan, F., et al., 2019. Superhydrophobic hemostatic nanofiber composites for fast clotting and minimal adhesion. Nat. Commun. 10 (1), 5562.

Liang, Y., He, J., Guo, B., 2021. Functional hydrogels as wound dressing to enhance wound healing. ACS Nano 15 (8), 12687–12722.

Maaz Arif, M., Khan, S.M., Gull, N., Tabish, T.A., Zia, S., Ullah Khan, R., et al., 2021. Polymer-based biomaterials for chronic wound management: Promises and challenges. Int. J. Pharm. 598, 120270.

Martínez-Pérez, D., Guarch-Pérez, C., Purbayanto, M.A.K., Choińska, E., Riool, M., Zaat, S.A.J., Wojciech, Ś., 2023. 3D-printed dual drug delivery nanoparticle- loaded hydrogels to combat antibiotic-resistant bacteria. Int. J. Bioprinting. 9 (3), 683.

Mendes, A.C., Gorzelanny, C., Halter, N., Schneider, S.W., Chronakis, I.S., 2016. Hybrid electrospun chitosan-phospholipids nanofibers for transdermal drug delivery. Int. J. Pharm. 510 (1), 48–56.

Miroshnikov, M., Kato, K., Babu, G., Divya, K.P., Arava, L.M.R., Ajayan, P.M., John, G., 2018. A common tattoo chemical for energy storage: henna plant-derived naphthoquinone dimer as a green and sustainable cathode material for Li-ion batteries. RSC Adv. 8 (3), 1576–1582.

Moazzami Goudarzi, Z., Soleimani, M., Ghasemi-Mobarakeh, L., Sajkiewicz, P., Sharifianjazi, F., Esmaeilkhanian, A., Khaksar, S., 2022. Control of drug release from cotton fabric by nanofibrous mat. Int. J. Biol. Macromol. 217, 270–281.

Montaser, A.S., Rehan, M., El-Senousy, W.M., Zaghloul, S., 2020. Designing strategy for coating cotton gauze fabrics and its application in wound healing. Carbohydr. Polym. 244, 116479.

Narayanan, G., Boy, R., Gupta, B.S., Tonelli, A.E., 2017. Analytical techniques for characterizing cyclodextrins and their inclusion complexes with large and small molecular weight guest molecules. Polym. Test. 62, 402–439.

Nicoletti CD, dos Santos Galvão RM, de Sá Haddad Queiroz M, Barboclher L, Faria AFM, Teixeira GP, et al. Inclusion complex of O-allyl-lawsone with 2-hydroxypropyl-β-cyclodextrin: Preparation, physical characterization, antiparasitic and antifungal activity. Journal of Bioenergetics and Biomembranes. 2023;55(3):233-48.

Ohene-Agyei, T., Mowla, R., Rahman, T., Venter, H., 2014. Phytochemicals increase the antibacterial activity of antibiotics by acting on a drug efflux pump. MicrobiologyOpen. 3 (6), 885–896. Epub 2014/09/17.

Olga, G., Styliani, C., Ioannis, R.G., 2015. Coencapsulation of ferulic and gallic acid in hp-b-cyclodextrin. Food Chem. 185, 33–40.

Patel, R.D., Raval, M.K., 2022. Differential scanning calorimetry: A screening tool for the development of diacerein eutectics. Results in Chemistry. 4, 100315.

Patil, S., Celebioglu, A., Uyar, T., 2023. Orally fast-dissolving drug delivery systems for pediatrics: Nanofibrous oral strips from isoniazid/cyclodextrin inclusion complexes. J. Drug Delivery Sci. Technol. 85, 104584.

Pinho, E., Soares, G., 2018. Functionalization of cotton cellulose for improved wound healing. J. Mater. Chem. B 6 (13), 1887–1898.

Qu, J., Zhao, X., Liang, Y., Zhang, T., Ma, P.X., Guo, B., 2018. Antibacterial adhesive injectable hydrogels with rapid self-healing, extensibility and compressibility as wound dressing for joints skin wound healing. Biomaterials 183, 185–199.

Rahmani, E., Çakici, A., Çakir, E., 2015. Antioxidant Activity and Phenolic Compounds of Lawson Molecule Extracted from Lawsonia inermis (Henna). International Journal of Food Engineering Research 7 (1), 1–16.

Rezaei, M., Davani, F., Alishahi, M., Masjedi, F., 2022. Updates in immunocompatibility of biomaterials: applications for regenerative medicine. Expert Rev. Med. Devices 19 (4), 353–367.

Safie, N.E., Ludin, N.A., Su'ait MS, Hamid NH, Sepeai S, Ibrahim MA, Teridi MAM., 2015. Preliminary study of natural pigments photochemical properties of curcuma longa l. and lawsonia inermis l. as tio 2 photoelectrode sensitizer. Malaysian Journal of. Anal. Sci. 19 (6), 1243–1249.

Sahtani, K., Aykut, Y., Tanik, N.A., 2022. Lawsone assisted preparation of carbon nanofibers for the selective detection of miRNA molecules. J. Chem. Technol. Biotechnol. 97 (1), 254–269.

Sakthiguru, N., Sithique, M.A., 2020. Preparation and In vitro biological evaluation of lawsone loaded o-carboxymethyl chitosan/zinc oxide nanocomposite for wound-healing application. Chem.Select 5 (9), 2710–2718.

Sandilya, A.A., Natarajan, U., Priya, M.H., 2020. Molecular View into the Cyclodextrin Cavity: Structure and Hydration. ACS Omega 5 (40), 25655–25667.

Saokham, P., Loftsson, T., 2017. γ-Cyclodextrin. Int. J. Pharm. 516 (1), 278–292.

Schneider, H.-J., Hacket, F., Rudiger, V., Ikeda, H., 1998. NMR studies of cyclodextrins and cyclodextrin complexes. Chem. Rev. 98 (5), 1755–1785.

Singh, D.K., Luqman, S., Mathur, A.K., 2015. Lawsonia inermis L.-A commercially important primaeval dying and medicinal plant with diverse pharmacological activity: A review. Ind. Crop. Prod. 65, 269–286.

Sultana, T., Hossain, M., Rahaman, S., Kim, Y.S., Gwon, J.-G., Lee, B.-T., 2021. Multi-functional nanocellulose-chitosan dressing loaded with antibacterial lawsone for rapid hemostasis and cutaneous wound healing. Carbohydr. Polym. 272, 118482.

Thomas, H.C., 2011. Checklist for Factors Affecting Wound Healing. Adv. Skin Wound Care 24 (4).

Topuz, F., Uyar, T., 2020. Electrospinning of cyclodextrin nanofibers: The effect of process parameters. J. Nanomater. 2020, 1–10.

Wang, W., Li, X., Shi, F., Zhang, Z., Lv, H., 2023. Study on the preparation of EGCG-γ-Cyclodextrin inclusion complex and its drug-excipient combined therapeutic effects on the treatment of DSS-induced acute ulcerative colitis in mice. Int. J. Pharm. 630, 122419.

Zhou, F.-L., Gong, R.-H., Porat, I., 2009. Nanocoating on filaments by electrospinning. Surf. Coat. Technol. 204 (5), 621–628.